Broad-band Ultrasonic Spectrometry of C_iE_j/Water Mixtures. Precritical Behavior

K. Menzel, A. Rupprecht, and U. Kaatze*

Drittes Physikalisches Institut, Georg-August-Universität, Bürgerstr. 42-44, D-37073 Göttingen, Germany

Received: October 31, 1996[⊗]

Between 0.1 and 2000 MHz the ultrasonic absorption spectra and sound velocities of the mixtures of water with some poly(ethylene glycol) monoalkyl ethers have been measured as a function of mole fraction in the complete composition range. The organic constituents are C_2E_1, *i*-C_3E_1, and C_4E_2. The results are discussed together with previous results for C_4E_1/water mixtures. The absorption spectra show attributes of relaxation time distribution which can be accounted for by the assumption of the Romanov−Solov'ev model of precritical concentration fluctuations. Debye-type relaxation terms which additionally exist in some spectra are tentatively related to mechanisms of C_iE_j dimerization by hydrogen bonding and also by hydrophobic interaction. The classical part of the absorption coefficient is evaluated to determine the volume-to-shear viscosity ratio and the sound velocity to obtain the adiabatic compressibility of the liquids. These quantities are also discussed in terms of hydrogen bond network characteristics of the mixtures of different composition.

1. Introduction

The detailed knowledge of the molecular behavior of aqueous nonelectrolyte solutions is of considerable significance, both for our understanding of fundamental characteristics of associating liquids, as well as for many applications in chemical engineering, environmental technology, food production, and various other topics of current wide interest. For this reason, numerous systematic studies of the properties of aqueous solutions of organic cosolvents have been performed in the past. Nevertheless, the molecular structure and dynamics of these fascinatingly complex liquids are still incompletely known. Particularly insufficient is our knowledge of mixtures at low water content.

More recently, evidence of a microheterogeneous structure of a variety of macroscopicly homogeneous mixtures has attracted attention. The particular shape of dielectric spectra of carboxylic acid/water mixtures, for example, has been discussed assuming the existence of two subphases, one with high and the other one with low water content.[1] Ultrasonic absorption spectra of mixtures of water with monohydric alcohols also indicate a microheterogeneous structure of the liquids. It is, however, not clear to what extent the special features of these spectra are due to fluctuations in the concentration[2] or to viscous and thermal conductivity effects at the internal boundaries between different subphases of the liquid.[3]

The formation of molecular clusters in mixtures of water with nonelectrolytes sensitively depends on the delicate balance between different interactions at hydrogen bonding sites on the one hand and hydrophobic parts of the molecule on the other hand. By simply changing the length of the hydrocarbon chain (C_i) and of the ethylene oxide part (E_j) of the organic molecule, this balance can be favorably adjusted if mixtures of water with alkyl polyglycol ethers (C_iE_j) are studied. Such mixtures thus offer optimum conditions to consider the interesting aspects of microheterogeneity in a multitude of binary liquids including micellar solution and systems with a miscibility gap.[4,5] We therefore decided to perform systematic studies of the ultrasonic absorption spectra of various C_iE_j/water mixtures. In view of the extreme sensitivity of ultrasonic absorption spectroscopy to a multitude of phenomena and in view of the useful information about molecular processes that is accessible by this method, various acoustical relaxation studies on C_iE_j/water mixtures have been performed in the past.[6−13] Despite the important insights in the binary systems that have been obtained from these studies, the frequency range of measurements was too small to allow for clear-cut conclusions on the underlying molecular processes reflected by the spectra. We therefore decided to perform a systematic study on C_iE_j/water mixtures based on broad-band ultrasonic absorption spectrometry in order to enable more definite statements on potential mechanisms under consideration.

In this paper we report on results of ultrasonic measurements at frequencies between 100 kHz adn 2 GHz on mixtures that do not show a miscibility gap. The poly(ethylene glycol)-monoalkyl ethers include C_2E_1, *i*-C_3E_1, and C_4E_2. Also considered are data for the systems C_4E_1/water that had been measured previously[14] at a temperature far below the lower critical temperature. These broad-band measurements aim particularly at an elucidation of the nature of the thermally activated molecular processes proceeding on precritical conditions and at their interactions with compressional waves. For this reason attempts are made to discuss the spectra in terms of various theoretical models, including stoichiometrically defined mechanisms of association, concentration fluctuations, and scattering processes that might occur in the microheterogeneous liquids.

2. Experimental Section

Sonic Absorption Spectrometry. The acoustic absorption coefficient α of the liquid samples has been measured as a function of frequency ν using two well-tried different methods.[15] At low frequencies, where α is small, a resonator technique has been applied where the path of interaction of the sound wave with the sample under test is virtually increased by multiple reflections. The liquid was contained in a biplanar cavity and the attenuation coefficient was determined from the quality factor of the cell. In order to account for instrumental loss it is necessary to perform reference measurements in which the cell is filled with a liquid of well-known properties. Hence α is actually measured relative to the attenuation coefficient α_r of a reference. In order to avoid mismatch in the configuration of the sonic field and in the acoustic impedance of the cavity when the sample is exchanged for the reference, close agreement

[⊗] Abstract published in *Advance ACS Abstracts,* January 15, 1997.

S1089-5647(96)03433-5 CCC: $14.00

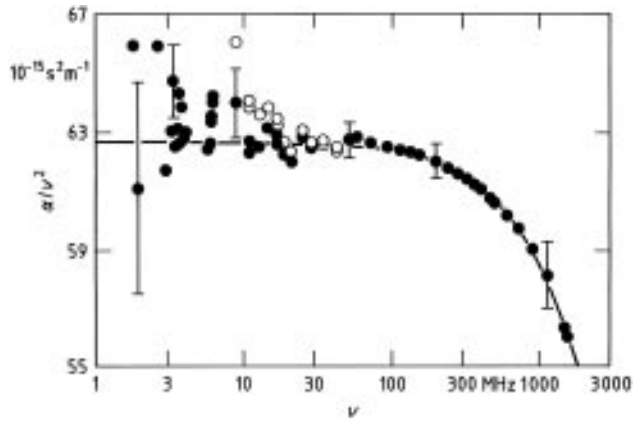

Figure 1. The absorption coefficient α per ν^2 as a function of frequency ν for the C_2E_1/H_2O mixture with mole fraction of ether $x = 0.6$ at 25 °C. Open symbols indicate pulse-modulated travelling wave transmission data before being corrected for diffraction effects. The curve is the graph of the relaxation spectral function defined by eq 8 with the parameter values given in Tables 3 and 4.

in the sound velocity and density of both liquids is required. Methanol/water mixtures of suitable composition have been preferably used as reference liquids here.

The resonance curves may be affected by spurious higher order (radial) modes[17,18] and, at high attenuation coefficient α, also by overlaps from neighboring main resonance peaks. To properly account for these disturbances we always measured the complete transfer function under consideration around a resonance peak under consideration and derived the resonance frequency and half-power bandwidth from a multipoint fit of the scan to the theoretical predictions.[19] We used two resonator cells. One with fundamental transducer frequency $\nu_T = 1$ MHz, cell diameter $2R_r = 70$ mm, and cell length $l_r = 14$ mm was utilized between 100 kHz and 3 MHz, and the other one ($\nu_T = 5$ MHz, $2R_r = 28$ mm, $l_r = 6$ mm) from 1.5 to 10 MHz.

At frequencies between 3 MHz and 2 GHz absolute measurements of α have been performed using a pulse-modulated travelling wave transmission method[15] in which the sample length x was varied in a computer-controlled mode of operation.[20] Three specimen cells, each matched to a particular frequency range, have been employed. These cells mainly differ from one another by the piezoelectric transmitter and receiver crystals. Between 3 and 60 MHz we used disc-shaped quarz transducers ($\nu_T = 1$ MHz, $2R_T = 40$ mm[20]). For measurements from 30 to 500 MHz, a cell with $LiNbO_3$ transducer discs ($\nu_T = 10$ MHz, $2R_T = 12$ mm) was available.[21] Using these cells the pair of transmitter/receiver crystals was operated at the odd overtones of the transducer fundamental frequency ($\nu_T(2n + 1)$; $n = 1, 2, ...$). Above 500 MHz broad-band end face excitation of $LiNbO_3$ rods ($2R_T = 3$ mm, length $l_T = 10$ mm) was applied[19,23] according to the method by Bömmel and Dransfeld.[22] Despite the complicated structure of the sound field radiated from a piston source,[24,25] on many conditions the transfer function $T(x)$ of the cells can nevertheless be represented assuming plane wave conditions. It is necessary for this purpose that the active receiver area agrees with that of the transmitter. For our present cells it was found that only below 20 MHz a correction for diffraction effects was required. This correction may depend on a variety of parameters.[26] For simplification we used the empirical relation

$$|T(x)| = |T(x)|_{meas}\left(\exp\left(-\sqrt{\frac{x}{\beta A_r}}\right)\right)^{g(x)} \qquad (1)$$

to convert measured transfer function data into the values $|T(x)|$ to be used in the evaluation procedure. In eq 1 A_r denotes the surface area of the transducers and $\beta = 2\pi/\lambda$ is the wave number of the sonic wave within the liquid. The weighing function $g(x)$ has been found by calibration measurements using water as reference liquid. The effect of correction for diffraction losses is illustrated by Figure 1.

TABLE 1: Relative Errors in the Attenuation Coefficient (α) and Sound Velocity (c_s) Data

ν, MHz	0.1−0.6	0.6−1.5	1.5−3	3−30	30−200	200−2000
$\Delta\alpha/\alpha$	0.06	0.04	0.07	0.02	0.01	0.02
$\Delta c_s/c_s$		0.001		0.0005	0.0005	0.0015

TABLE 2: Mass Fraction (y), Mole Fraction (x), and Concentration (c) of the Organic Constituent as well as Density (ρ), Sound Velocity at Low Frequencies[a] (c_{so}), and Static Shear Viscosity[b] (η_s) of the Mixtures at 25 °C

y ± 0.1%	x ± 0.1%	c mol/L, ±0.2%	ρ g/cm^3, ±0.2%	c_{so} m/s, 0.1%	η_s 10^{-3} Pa·s, ±2%
			C_2E_1		
0.303	0.080	3.36	0.998	1646	2.09
0.469	0.150	5.16	0.992	1615	3.00
0.556	0.200	6.08	0.985	1577	3.26
0.625	0.250	6.79	0.979	1541	3.37
0.706	0.324	7.60	0.970	1496	3.27
0.882	0.600	9.25	0.945	1385	2.63
1.000	1.000	10.33	0.931	1302	1.71
			i-C_3E_1		
0.091	0.017	0.87	0.995	1561	1.20
0.194	0.040	1.85	0.994	1614	1.70
0.335	0.080	3.17	0.989	1605	2.51
0.391	0.100	3.68	0.985	1584	2.82
0.505	0.150	4.70	0.974	1532	3.37
0.591	0.200	5.44	0.965	1492	3.65
0.853	0.500	7.53	0.928	1361	3.32
1.000	1.000	8.55	0.899	1269	2.01
			C_4E_1		
0.085	0.014	0.72	0.994	1553	1.35
0.100	0.017	0.84	0.994	1554	1.43
0.170	0.030	1.42	0.989	1528	1.80
0.200	0.037	1.66	0.986	1521	2.02
0.220	0.041	1.83	0.981	1514	2.14
0.275	0.055	2.28	0.981	1503	2.45
0.295	0.060	2.44	0.977	1496	2.57
0.315	0.065	2.60	0.976	1491	2.71
0.370	0.082	3.04	0.970	1478	3.02
0.400	0.092	3.28	0.968	1471	3.16
0.580	0.174	4.66	0.950	1432	3.98
0.740	0.303	5.86	0.935	1401	4.52
1.000	1.000	7.59	0.897	1306	2.79
			C_4E_2		
0.121	0.015	0.74	0.994	1568	1.35
0.155	0.020	0.96	0.999	1569	1.51
0.218	0.031	1.38	0.999	1560	1.89
0.273	0.040	1.68	0.997	1553	2.29
0.500	0.100	3.05	0.990	1518	4.36
0.807	0.300	4.76	0.973	1447	6.66
0.931	0.600	5.50	0.958	1392	5.89
1.000	1.000	5.85	0.948	1358	4.59

[a] The c_{so} values refer to measurements at frequencies around 1 MHz. [b] The shear viscosity has been measured with a falling ball viscometer except the C_4E_1 values which have been derived from literature data[27,28] by interpolation.

Sound Velocity. At frequencies between 100 kHz and 10 MHz the sound velocity c_s of the sample has been obtained as a byproduct of the α-measurements using resonator cells. It has been determined from the cell resonance frequencies of successive peaks. In doing so, the nonequidistant distribution of the resonance frequency has been carefully taken into account.[15,18] We did, however, not consider possible small effects from the finite cell radius and from the sample attenuation coefficient when calculating c_s. At higher frequencies

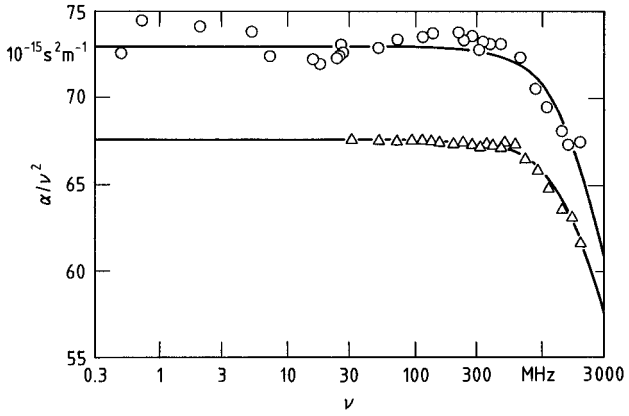

Figure 2. Sonic absorption spectra for pure C_4E_1 (circles) and *i*-C_3E_1 (triangles) at 25 °C. The curves represent the Debye-type spectrum defined by eq 3 with the parameter values found by the fitting procedure Table 3 and 4.

sound velocity data were available from the waviness in the signal transmitted through the cell as resulting from multiple reflections at small transducer spacing. To allow for accurate measurements of the wavelength λ within the sample thereby, a pulse duration $T = 3$ μs has been used.

Experimental Errors. The measuring frequency was known and kept constant during the measurements with a negligible error throughout. The temperature of the cells and a possibly existing temperature gradient within the sample volume has been measured with the aid of a Pt-100 resistance thermometer (±0.01 K), which had been calibrated against a high-precision mercurial thermometer. Depending on the particular cell construction, errors in the temperature of the sample vary between 0.02 and 0.05 K, resulting in an error of less than 0.1% in the α-values. Care has been taken to avoid changes in the concentration of the mixtures by preferential evaporation of one constituent, for example. Repeated measurements have been performed with all samples. No noticeable changes of the α- and c_s-values have been found.

Errors in the data measured with resonator cells are predominantly due to the need for a calibration measurement. Small changes in the adjustment of the cell during the cleaning and refilling procedure when the sample is exchanged for a reference liquid results in an experimental uncertainty that depends significantly on the α-values of the sample itself. At small α the error in the attenuation coefficient is particularly high since the half-power bandwidth of the resonance curve is mainly given by the instrumental loss. At frequencies between 3 and 500 MHz the accuracy of the α-data determined by the pulse-modulated travelling wave transmission method is mainly restricted by the nonperfect parallelism of the transmitter and receiver crystal faces and by the incomplete consideration of diffraction effects. At higher frequencies where the maximum usable transducer spacing may be as small as 6 μm the insufficient knowledge of the sample thickness (±100 nm) is the limiting factor in the accuracy of the measurements. In total, the errors listed in Table 1 have to be taken into account when evaluating the data.

Binary Mixtures. 2-Ethoxyethanol (C_2E_1) was purchased from Fluka (Neu-Ulm, FRG, >99.5%), 2-Isopropoxyethanol (*i*-C_3E_1), 2-Butoxyethanol (C_4E_1), and 2-(2-butoxyethoxy)ethanol (C_4E_2) were purchased from Aldrich (Steinheim, FRG >99%). All poly(ethylene glycol)monoalkyl ethers were used without additional purification. Water was distilled and deionized by mixed-bed ion exchange. The mixtures were prepared by weighing appropriate amounts of the constituents into suitable flasks. A survey of the liquids measured in this study is presented in Table 2 where besides concentration data the density ρ, the low-frequency sound velocity c_{so}, and the static shear viscosity η_s of the liquids are given. For reasons of completeness the system C_4E_1/H_2O is also included in this table.

TABLE 3: Parameters in the Romanov−Solov'ev Term in Eq 10 and *B*-Parameter of the Classical Part in the Absorption Spectra ($B = (\alpha\lambda)_{cl}/\nu$, Eq 4) for C_iE_j/H_2O Mixtures at 25 °C

y	A_{RS} 10^{-3}, ±20%	τ_{RS} ns, ±15%	B ps, ±2%
	C_2E_1		
0.303	30	0.09	48.6
0.469	61	0.15	71.7
0.556	67	0.14	79.0
0.625	65	0.12	81.5
0.706	62	0.08	78.1
0.882	14	0.03[a]	69.2
1.000			45[a]
	i-C_3E_1		
0.091	1.6	0.1[a]	35.3
0.194	16	0.15	43.7
0.335	51	0.51	62[a]
0.391	51	0.63	71.1
0.505	50	0.56	80.8
0.591	40	0.49	87.5
0.853	23	0.1[a]	69.1
1.000			56.4
	C_4E_1		
0.085	2.5	4.3[a]	37.2
0.100	17	4.3	37.7
0.170	85	4.3	44.4
0.200	87	3.3	46.8
0.220	85	2.9	49.7
0.275	82	2.2	51.7
0.295	80	1.9	55.6
0.315	75	1.9	57.1
0.370	62	1.6	63.0
0.400	64	1.29	61.8
0.580	35	0.95	74.4
0.740	23	0.57	76.7
1.000			68.7
	C_4E_2		
0.121	6.6	2.0	39.0
0.155	29	2.1	41.0
0.218	66	1.7	47.1
0.273	96	1.5	52.1
0.500	92	0.67	68.8
0.807	18	0.49	104.0
0.931	1.1	0.2[a]	102[a]
1.000			100[a]

[a] This value has been fixed in the final run of the fitting procedure.

3. Results and Analytical Description of Measured Spectra

Pure C_iE_j. In Figure 2 the sonic absorption coefficient α divided by ν^2 is displayed as a function of frequency ν for two alkyl polyglycol ethers. In contrast to water, for which $\alpha/\nu^2 =$ const ($=B/c_s = 21.24 \cdot 10^{-15}$ s^2 m^{-1}, 25 °C), a dispersion is found in the frequency range around 1 GHz. Hence the sound attenuation per wavelength, $\alpha\lambda$, of the organic liquids is not just given by a classical term

$$(\alpha\lambda)_{cl} = B\nu \qquad (2)$$

but reflects relaxation characteristics. Since, on the other hand, the α/ν^2 data (Figure 2) do not reach a constant high-frequency value within the frequency range of measurement, the type of the underlying relaxation spectral function cannot be derived from the measured data. We therefore represent the spectra of the C_iE_j by the simplest relaxation spectral function:

$$\alpha\lambda = \frac{A_D \omega\tau_D}{1 + (\omega\tau_D)^2} + (\alpha\lambda)_{cl} \quad (3)$$

In the Debye-type[29] relaxation spectral term (D) on the right hand side of eq 3 τ_D denotes a discrete relaxation time, A_D is an amplitude ($\alpha\lambda - (\alpha\lambda)_{cl} = A_D/2$ at $\omega = \tau_D^{-1}$), and $\omega = 2\pi\nu$. The results for the parameters of the function 3 as found by a nonlinear least-squares regression analysis are included in Tables 3 and 4, respectively. Here and in what follows a theoretical relaxation spectral function $R(\nu_n; \xi_1, ..., \xi_P)$ has been fitted to the measured spectra (ν_n) using a Marquardt algorithm[30] that minimizes the variance:

$$\chi^2(\xi_1, ..., \xi_P) = \frac{1}{N - P - 1}\sum_{n=1}^{N} w(\nu_n)|Y(\nu_n) - R(\nu_n; \xi_1, ..., \xi_P|^2 \quad (4)$$

Herein ν_n, $n = 1, ..., N$, denote the frequencies of measurement, and $w(\nu_n) = \Delta Y^{-1}(\nu_n)$ are weighing factors. The uncertainties in the values of the parameters $\xi_p = 1, ..., P$, have been derived from additional runs in which sets of pseudodata $\tilde{Y}(\nu_n)$ were used in the fitting procedure. These $\tilde{Y}(\nu_n)$ data have been generated by adding, within the limits of experimental error $\pm\Delta Y(\nu_n)$, Table 1, random values to the measured data.

Mixtures with Water. As illustrated by the example shown in Figure 1 the measured α/ν^2 data of the C_iE_j/water mixtures exhibit also relaxation characteristics. We found, however, that the spectra of the binary liquids cannot be adequately represented by a discrete relaxation time. It turned out that, within their limits of experimental error, the spectra of all mixtures of water with C_2E_1, *i*-C_3E_1, and C_4E_2 can be well represented by a sum of a restricted Hill[31−33] relaxation term and the classical contribution:

$$\alpha\lambda = \frac{A_H \omega\tau_H}{(1 + (\omega\tau_H)^{2s_H})^{3/(4s_H)}} + (\alpha\lambda)_{cl} \quad (5)$$

The restricted Hill term (H) results from the original form

$$R_H(\nu) = \frac{A_H(\omega\tau_H)^{m_H}}{(1 + (\omega\tau_H)^{2s_H})^{(m_H+n_H)/(2s_H)}} \quad (6)$$

if the relaxation time distribution parameters m_H and n_H are fixed at $m_H = 1$ and $n_H = 0.5$. Hence the sonic absorption spectra of three series of binary mixtures can be represented just by the four parameters A_H, τ_H, s_H, and B (Figure 3), where s_H determines the shape of the spectral function around $\nu_r = (2\pi\tau_H)^{-1}$.

As shown by the example displayed in Figure 4, the spectra for the C_4E_1/water system exhibit two shoulders, indicating that there exist at least three relaxation processes. It has already been shown previously[14] that the sonic absorption spectra of this series of mixtures can be well represented if, in addition to a restricted Hill term and the classical contribution, a low-frequency (Dl) and a high-frequency (Dh) Debye term are considered in eq 5:

$$\alpha\lambda = \frac{A_{Dl}\omega\tau_{Dl}}{1 + (\omega\tau_{Dl})^2} + \frac{A_H\omega\tau_H}{(1 + (\omega\tau_H)^{2s_H})^{3/(4s_H)}} + \frac{A_{Dh}\omega\tau_{Dh}}{1 + (\omega\tau_{Dh})^2} + (\alpha\lambda)_{cl} \quad (7)$$

TABLE 4: Parameters of the Low (*l*) and High (*h*) Frequency Debye Term, Respectively, in the Model Relaxation Spectral Function (Eq 8) for C_iE_j/H_2O Mixtures at 25 °C

y	$A_{Dl}\ 10^{-3}$, ±20%	τ_{Dl} μs, ±20%	$A_{Dh}\ 10^{-3}$, ±20%	τ_{Dh} ns, ±20%
		C_2E_1		
0.882			17	0.1[a]
1.000			87	0.04
		i-C_3E_1		
0.335			50	0.25
0.391			78	0.27
0.505			98	0.23
0.591			93	0.21
0.853			100[a]	0.06
1.000			100[a]	0.05
		C_4E_1		
0.085	1.6	0.004	1.5	1[a]
0.100	11	0.04	5.3	0.88
0.170	7.3	0.09	24	0.79
0.200	11	0.08	29	0.62
0.220	10	0.07	33	0.67
0.275	13	0.06	39	0.51
0.295	15	0.06	39	0.48
0.315	12	0.06	45	0.48
0.370	14	0.05	50	0.48
0.400	11	0.04	52	0.37
0.580	3.3	0.03	64	0.29
0.740	0.8	0.012	68	0.18
1.000			70[a]	0.06
		C_4E_2		
0.121	2.2	0.007	4.6	0.6[a]
0.155	13	0.012	10	0.5[a]
0.218	19	0.008	19	0.44
0.273	6.3	0.008	27	0.4[a]
0.500			53	0.21
0.807			72	0.21
0.931			71	0.15
1.000			68	0.10

[a] This value has been fixed in the final run of the regression analysis.

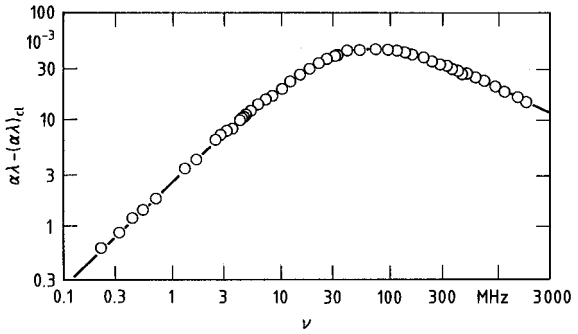

Figure 3. The sonic excess absorption per wavelength, $\alpha\lambda - (\alpha\lambda)_{cl}$, versus frequency ν for the C_4E_2/H_2O mixture with mole fraction $x = 0.04$ of ether at 25 °C. The curve is the graph of the restricted Hill term as given by eq 5 with the parameter values obtained by the regression analysis of the measured data.

Functions 5 and 7 allow the measured spectra to be analytically represented by a minimum number of adjustable parameters, respectively. These empirical functions also enable some conclusions on underlying molecular mechanisms.[19,23] We nevertheless additionally applied relaxation functions which are based on physical models of the liquid structure and microdynamics of the mixtures. Among the functions considered has been a sum of *k* Debye terms ($k = 1, 2, ...$) representing chemical relaxations, expressions that reflect dissipation of sound energy at internal interfaces of microheterogeneous samples,[34−38] and particularly relations that result from the assumption of concentration fluctuations in binary mixtures[39−51] including a jump-

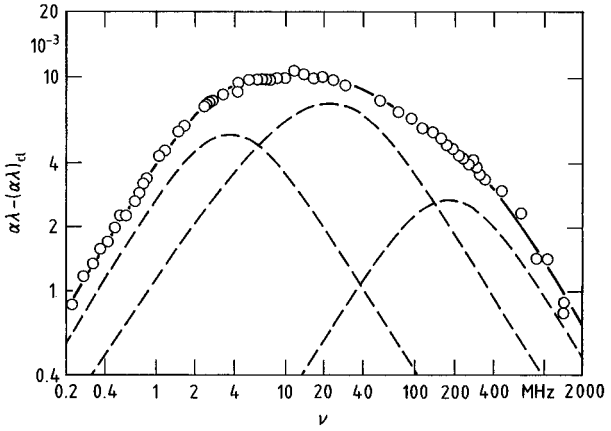

Figure 4. Example for a more complicated excess absorption spectrum: data for the C_4E_1/water mixture with mole fraction $x = 0.017$ of ether at 25 °C. The full curve represents the spectrum as defined by eq 8 with the parameter values given in Tables 3 and 4. The dashed curves indicate the subdivision of the spectrum in two Debye terms and a Romanov−Solov'ev term.

diffusion model.[52,53] We found the smallest values in the variance χ^2, combined with a self-consistent dependence of the parameter values ξ_1, ..., ξ_P on the mixture composition, if the model spectral function

$$\alpha\lambda = \frac{A_{Dl}\omega\tau_{Dl}}{1+(\omega\tau_{Dl})^2} + A_{RS}\omega\tau_{RS}I(\omega\tau_{RS}) + \frac{A_{Dh}\omega\tau_{Dh}}{1+(\omega\tau_{Dh})^2} + (\alpha\lambda)_{cl} \quad (8)$$

was used. The second term on the right-hand side of this equation represents the Romanov-Solov'ev relaxation of sound attenuation by noncritical, noncorrelated fluctuations in the mixture concentration.[41,42,44] Again, A_{RS} denotes an amplitude,

$$\tau_{RS} = l_m^2/D \quad (9)$$

is a diffusion time, and I is a scaling function which can be written in an explicite form:

$$I(\omega\tau_{RS}) = 3 - \frac{3\sqrt{\omega\tau_{RS}}}{4\sqrt{2}}\left[2\pi - ln\frac{\omega\tau_{RS} - \sqrt{2\omega\tau_{RS}} + 1}{\omega\tau_{RS} + \sqrt{2\omega\tau_{RS}} + 1} - 2\arctan(\sqrt{2\omega\tau_{RS}} + 1) - 2\arctan(\sqrt{2\omega\tau_{RS}} - 1)\right] \quad (10)$$

In eq 9 l_m is a minimum interaction length of fluctuations at thermal equilibrium and D is the mutual diffusion coefficient.

The regression analysis yielded a Romanov−Solov'ev term in the spectra of all C_iE_j/water mixtures under consideration. The values of the amplitude A_{RS} and the diffusion time τ_{RS} as well as for the B-parameter of the classical contribution are collected in Table 3. The high-frequency Debye-type relaxation appeared to be also present in most liquids while the additional low-frequency Debye-term seems to exist in the spectra of the C_4E_1/water mixtures and in the C_4E_2/water mixtures of high water content only. The values of the amplitudes A_{Dl} and A_{Dh} and of the relaxation times τ_{Dl} and τ_{Dh} resulting from the fitting procedure are displayed in Table 4.

4. Discussion

Precritical Fluctuations. In Figure 5, the amplitude A_{RS} of the Romanov−Solov'ev term in the model spectral function (eq 8) is displayed as a function of mole fraction x of the C_iE_j. A_{RS} vanishes for the pure constituents and exhibits one clear relative maximum for each series of mixtures. That smallest width in the A_{RS} peak is found with the C_4E_1/water system that exhibits a miscibility gap at high temperatures (Figure 6). The dependence of the relaxation amplitude upon x may be taken as another indication of the existence of concentration fluctuations. The τ_{RS}-values of the four series of binary mixtures (Table 3) also show a relative maximum. There do not appear, however, obvious relations between the x-values of the maxima and the chemical composition and structural properties of the poly(ethylene glycol) monoethyl ethers. For this reason, we used eq 9 along with diffusion coefficient data[54−57] from the literature (Figure 6) to calculate the minimum interaction length l_m for the C_4E_1/H_2O system. At low y the length l_m decreases to reach a nearly constant value above the critical composition y_c ($l_m \approx 4.4$ Å, $y_c < y < 0.8$).

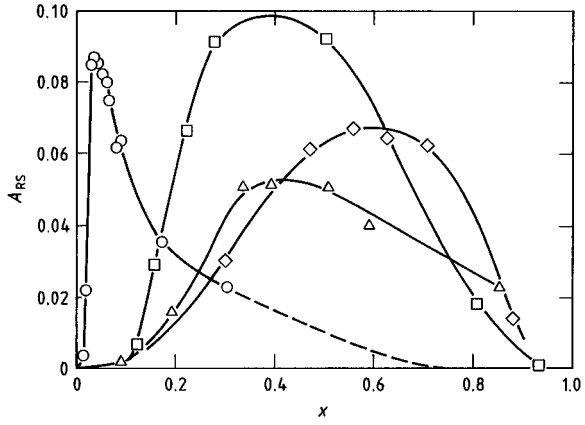

Figure 5. The amplitude A_{RS} of the Romanov−Solov'ev term in eq 8 versus mole fraction x of ether for the mixtures of water with C_2E_1 (◇), i-C_3E_1 (△), C_4E_1 (○), and C_4E_2 (□) at 25 °C.

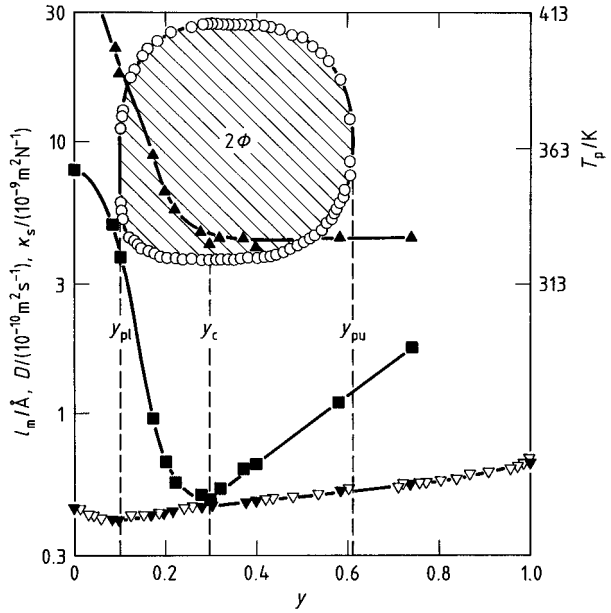

Figure 6. Plot of the minimum interaction length l_m (▲, eq 9), the mutual diffusion coefficient D (■[54−57]), and the adiabatic compressibility κ_s (▼, eq 11; ▽[59]) displayed as a function of mass function y of ether for the $C_4E_1//H_2O$ mixtures at 25 °C. Also shown to indicate the miscibility gap (hatched area) is the phase separation temperature T_p (○[58]). Here y_c denotes the lower critical mass fraction of the system and y_{pl}, y_{pu} the lowest and highest mass fraction, respectively, at which two phases exist.

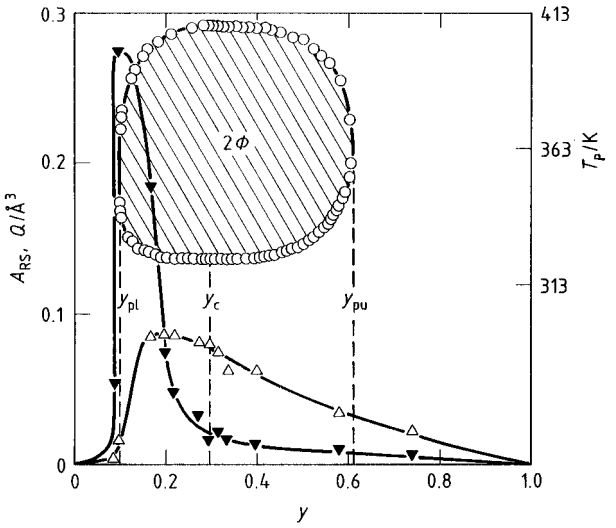

Figure 7. The amplitude A_{RS} (△; eq 8) and the quantity Q (▼, eq 12) of the Romanov−Solov'ev model at 25 °C shown for the C_4E_1/water mixtures as a function of mass fraction of ether. See Figure 6 for the phase separation temperature T_P.

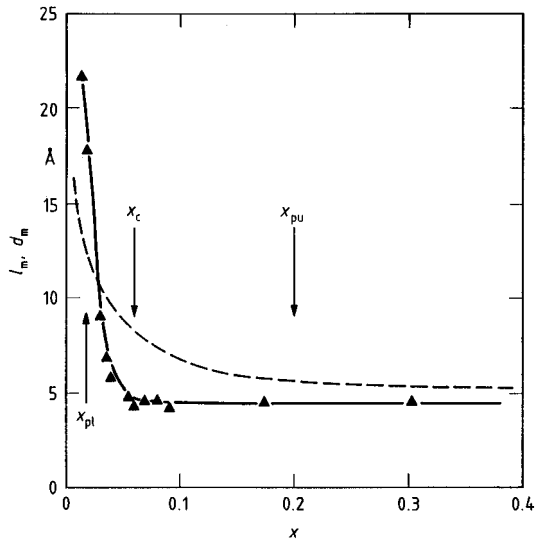

Figure 8. The minimum interaction length l_m (▲) and the mean distance d_m between C_4E_1 molecules (dashed curve; eq 14) for the C_4E_1/water mixtures at 24 °C plotted versus the mole fraction x of ether.

Also given in Figure 7 is the Q-parameter of the Romanov−Solov'ev model, which according to

$$Q = \frac{\rho c_s^{\,2} k_B T}{8\pi} \frac{V^2}{g''^2}\left(\frac{v''}{V} - \frac{A}{c_p} h''\right)^2 \tag{11}$$

is related to the second derivatives (with respect to the equilibrium mole fraction of the ethers) of the Gibbs free enthalpy (g''), the molar volume (v''), and the molar enthalpy (h''). In eq 11 is k_B the Boltzmann constant, V the molar volume, A is the instantaneous thermal expansion coefficient, and c_p the specific heat at constant pressure. Here, the Q values have been calculated from the amplitudes using the relation

$$Q = 3 l_m^{\,3} A_{RS} \tag{12}$$

The quantity Q exhibits a sharp relative maximum at y_{pl}. Hence, at this composition the v'' and the h'' term in eq 12 are far from compensating each other. Obviously, at least one of the derivatives v'', h'', or even g'' changes significantly at around y_{pl}.

The finding of a relative extremum at y_{pl} is not an unusual result. The apparent molal heat capacity, for example, also exhibits a sharp maximum at this particular mass fraction[60] while the adiabatic compressibility κ_s passes through a weak minimum at y_{pl} (Figure 6). The κ_s values have been derived from the sound velocity and density data as usual, assuming the relation

$$\kappa_s = c_s^{\,-2} \rho^{-1} \tag{13}$$

It is interesting to compare the data for the minimum interaction length l_m with the mean distance d_m between the C_4E_1 molecules in the mixture. For reasons of simplification let us assume the butoxyethanol molecules to be distributed on a cubic lattice and let us thus use the relation

$$d_m = (N_A c)^{1/3} \tag{14}$$

to estimate d_m values. Herein N_A denotes the Avogadro number. The minimum interaction length l_m seems to exceed d_m only around x_{pl} (Figure 8). At $0.033 < x$ a minimum interaction length smaller than d_m results. This finding may be taken to point at association of C_4E_1 molecules as discussed below.

Chemical Relaxations. Most C_iE_j/water mixtures, in addition to the Romanov−Solov'ev contribution that reflects precritical concentration fluctuations, exhibit one or two Debye terms in their ultrasonic absorption spectra. As usual these terms are assumed to be due to stoichiometricly well-defined processes. It is interesting to notice that the existence of additional Debye terms seems to be characteristic of hydrogen-bonding binary liquids with either critical demixing point[19,61,62] or precritical behavior.[2,51]

The high-frequency Debye term already exists in the spectra of the pure C_iE_j, with relaxation rates τ_{Dh}^{-1} in the small range between 10^{10} s^{-1} and $2 \cdot 10^{10}$ s^{-1}. Furthermore, the parameters of the high-frequency term smoothly vary when water is added to the pure poly(ethylene glycol)monoalkyl ethers. We thus suggest this term to reflect the same elementary chemical process in the mixtures as in the pure organic liquids. Since such process can be a reaction of C_iE_j molecules only it is an obvious attempt to assume a mechanism of structural isomerization:

$$C_iE_j \underset{k_r}{\overset{k_f}{\rightleftharpoons}} (C_iE_j)^* \tag{15}$$

or of dimerization:

$$2C_iE_j \underset{k_r}{\overset{k_f}{\rightleftharpoons}} (C_iE_j)_2 \tag{16}$$

The concentration dependence of the measured amplitudes A_{Dh} and relaxation rates τ_{Dh}^{-1} of the different series of C_iE_j/water mixtures shows a strikingly uniform behavior (Figure 9) but does not fit with either equilibrium as defined by eqs 15 and 16. Isomerization is expected to be governed by a relaxation rate[63]

$$\frac{1}{\tau} = k_f + k_r \tag{17}$$

independent of c. According to

$$\frac{1}{\tau} = (8 k_f k_r c + (k_r)^2)^{1/2} \tag{18}$$

the relaxation rate of a dimerization reaction follows a more complicated concentration dependence than the linear relation displayed in Figure 9.

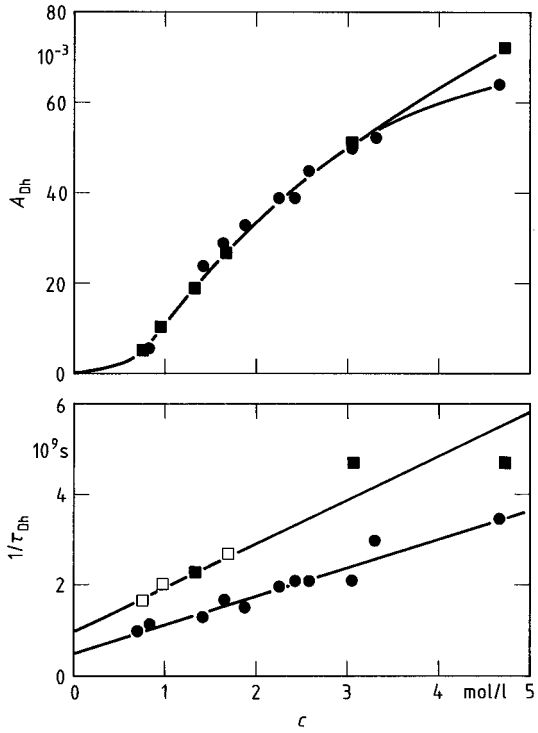

Figure 9. Amplitude A_{Dh} and relaxation rate τ_{Dh}^{-1} of the high-frequency Debye term at 25 °C plotted versus the ether concentration c for mixtures of water with C_4E_1 (points) and C_4E_2 (box; open symbols denote values that have been fixed in the fitting procedure).

The discrepancy between the concentration dependence in the parameters of the measured spectra and the predictions from the principles of chemical kinetics may be due to various imperfections. Most likely it is predominantly a reflection of the physically incorrect trends in the high-frequency part ($\nu > (2\pi\tau_{RS})^{-1}$) of the Romanov−Solov'ev function. Hence, no definite conclusion on the underlying mechanism of the high-frequency Debye term can be drawn from the sonic spectra.

In normal alkanes structural isomerization leads to Debye-type ultrasonic excess absorption with relaxation times that increase from 0.08 to 0.27 ns when going from *n*-decane to *n*-hexadecane (25 °C[64]). These data are in fair accordance to the τ_{Dh} data for the pure C_iE_j ($\tau_{Dh} \leq 0.1$ ns, Table 4). On the other hand, however, pure carboxylic acids reveal a high-frequency relaxation with relaxation time between 0.13 and 0.6 ns, reflecting the monomer/open dimer reaction of the carboxyl groups.[62] Hence, from those results the high-frequency Debye relaxation in the spectra of the pure C_iE_j and also of the C_iE_j/water mixtures might be due to dimerization by hydrogen bonding.

The low-frequency Debye term does exist neither in the spectra of pure C_iE_j nor in those for mixtures of C_2E_1 and *i*-C_3E_1 with water (Table 4). Both series of spectra for the mixtures of the more oleophilic C_4E_1 and C_4E_2 with water exhibit a relative maximum in the relaxation amplitude. It is, therefore, suggested that the low-frequency relaxation term reflects one special step within the concentration fluctuation kinetics of the mixtures, most likely a dimerization by hydrophobic interaction. Effects of hydrophobic dimerization are expected to increase with the length of the oleophilic part of the organic molecule. These effects involve a rearrangement of the (hydrophobic) hydration water and are thus expected to depend on the concentration of both constituents of the microheterogeneous mixtures.

Volume Viscosity and Shear Viscosity. If small effects of heat conduction are neglected the classical contribution to the sound absorption per wavelength, according to the equation[65]

$$(\alpha\lambda)_{cl} = B\nu = \frac{2\pi^2\nu\eta_s}{\rho c_s^2}\left(\frac{\eta_\nu}{\eta_s} + \frac{4}{3}\right) \qquad (19)$$

is related to the shear viscosity η_s and the volume viscosity η_ν of the liquids. Supposing the *B*-values found in our fitting procedure (Table 3) to correctly represent the classical part, hence assuming no contributions from further high-frequency chemical relaxations to exist in the $(\alpha\gamma)_{cl}$ term of the model spectral function defined by eq 8, the η_ν/η_s ratios of the C_iE_j/water systems have been evaluated and displayed in Figure 10. As shown by this diagram the η_s/η_ν values significantly decrease from the pure water value ($\eta_\nu/\eta_s = 2.68$, $y = 0$, 25 °C) when poly(ethylene glycol)monoalkyl ethers are added. The high η_ν/η_s value for pure water is assumed to be due to the voluminous hydrogen-bonded water structure.[65,66] Obviously, this structure is successively destroyed on addition of the organic molecules. Pure *i*-C_3E_1, C_4E_1, and C_4E_2 reveal η_ν/η_s values close to 2/3, as assumed a reasonable estimate for liquids without particular characteristics.[67,68] C_2E_1 shows a somewhat higher η_ν/η_s value than the other ethers, indicating that there seems to exist a noticeable effect of association in the smallest homologue. However, with all C_iE_j systems the η_ν/η_s ratio decreases when water is added to the ethers. This finding may be taken to indicate that also with the higher homologues there exists a particular liquid structure that partly breaks down on addition of water.

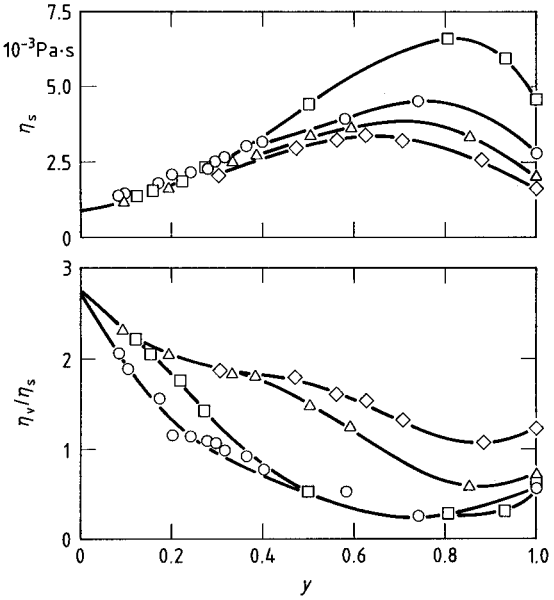

Figure 10. Shear viscosity η_s (Table 2) and volume-to-shear viscosity ratio η_ν/η_s (eq 19) at 25 °C shown as a function of mass fraction of ether for mixtures of water with C_2E_1 (◇), *i*-C_3E_1 (△), C_4E_1 (○), and C_4E_2 (□).

On a first glance this relative minimum in the η_ν/η_s versus y relations seem to contradict the relative maximum in the η_s versus y curves (Figure 10) and also the dependence of the characteristic dielectric relaxation time $\hat{\tau}$ of poly(ethylene glycol)monoalkyl ether/water mixtures upon mixture composition.[69−71] Water molecules that are added to pure ethers or their mixtures of low water content, obviously are preferably incorporated as hydrogen-bonded links between ether groups of the organic molecules.[69−71] The motions of these ether groups are slowed down by such links. The reduction in the volume viscosity shows that this association via water bridges leads to a somewhat more dense structure rather than a more voluminous hydrogen bond network.

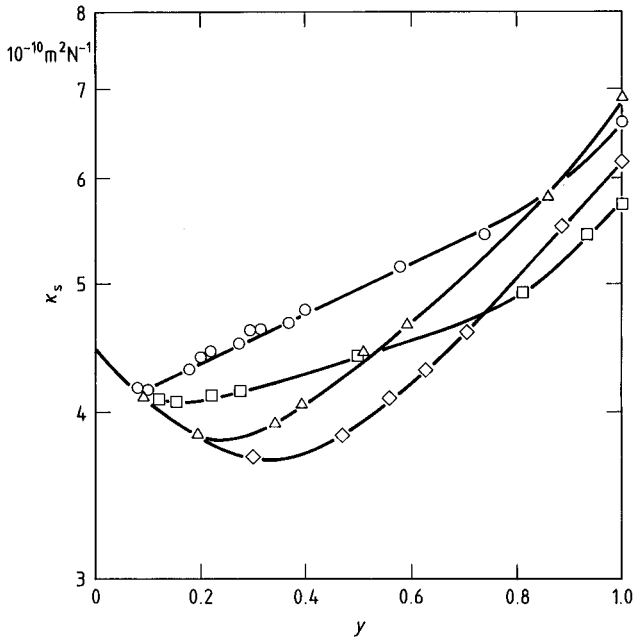

Figure 11. The adiabatic compressibility κ_s (eq 11) versus mass fraction y of ether for the C_iE_j/water mixtures at 25 °C (◇, C_2E_1; △, *i*-C_3E_1; ○, C_4E_1; □, C_4E_2).

We are aware that the relative minima in the η_ν/η_s data may at least in parts also result from a prospective dispersion in the shear viscosity ($d\eta_s/d\nu < 0$) of the liquids that has not been considered here. The existence of such shear viscosity dispersions in the current frequency range of measurements has been established recently by ultrasonic absorption[72] and shear wave spectrometry[73] of some alcohols.

Adiabatic Compressibility. In Figure 11 the isentropic compressibility κ_s of the liquids as following from the relation 13 is displayed as a function of mass fraction y. The κ_s values also decrease from the water value ($\kappa_s = 4.4773 \cdot 10^{-10}$ m^2 N^{-1}, $y = 0$, 25 °C) when C_iE_j is added, again reflecting the successive breakdown of the voluminous water structure. The compressibility of the pure C_iE_j, however, is even distinctly higher than that of water (e.g., $\kappa_s = 5.74 \cdot 10^{-10}$ m^2 N^{-1}, C_4E_2; $\kappa_s = 6.95 \cdot 10^{-10}$ m^2 N^{-1}, *i*-C_3E_1; 25 °C), and it decreases on addition of water. This result points also at a more voluminous C_iE_j structure that shrinks when water molecules are incorporated as hydrogen-bonding links.

5. Conclusions

The acoustic properties of C_iE_j/water mixtures provide useful information on the structure and microdynamics of the associating binary liquids. The concentration dependences of parameters such as the adiabatic compressibility and the volume viscosity to shear viscosity ratio do not show unusual characteristics but indicate the reorganization of the hydrogen bond network as a function of mixture composition. The sonic absorption spectra reveal attributes of relaxation time distribution which can be consistently complied with the assumption of a microheterogeneous liquid structure driven by precritical concentration fluctuations. An additional low-frequency Debye-type relaxation term in some spectra of water with C_4E_1 and C_4E_2 points at a mechanism of hydrophobic association, most probably of dimerization of C_iE_j molecules. A high-frequency Debye-type relaxation process with relaxation time between 50 and 900 ps exists in the pure C_iE_j and in the C_iE_j rich mixtures. This process is likely to reflect the dimerization of the poly(ethylene glycol)monoalkyl ethers by hydrogen bonding. However, the concentration dependences of the relaxation times and relaxation amplitudes do not sufficiently well agree with the predictions from chemical kinetics equations. This finding seems to predominantly result from the wrong high-frequency characteristics of the Romanov−Solov'ev spectral function used to describe the contributions from concentration fluctuations to the sonic absorption.

6. Acknowledgements

We are indebted to Professor R. Pottel and Dr. V. Kühnel for many discussions. Financial support by the Deutsche Forschungsgemeinschaft is gratefully acknowledged.

References and Notes

(1) Kaatze, U.; Menzel, K.; Pottel, R. *J. Phys. Chem.* **1991**, *95*, 324.
(2) Brai, M.; Kaatze, U. *J. Phys. Chem.* **1992**, *96*, 8946.
(3) Kaatze, U.; Brai, M.; Menzel, K. *Ber. Bunsen-Ges. Phys. Chem.* **1994**, *98*, 1.
(4) Degiorgio, V.; Corti, M., Eds. *Physics of Amphiphiles: Micelles, Vesicles and Microemulsions*; North-Holland: Amsterdam, 1985.
(5) Schick, M. J., Ed. *Nonionic Surfactants, Physical Chemistry*; Marcel Dekker: New York, 1987.
(6) Nishikawa, S.; Tanaka, M.; Mashima, M. *J. Phys. Chem.* **1981**, *85*, 686.
(7) Nishikawa, S.; Uchida, T. *J. Solution Chem.* **1983**, *12*, 771.
(8) Nishikawa, S.; Kotegawa, K. *J. Phys. Chem.* **1985**, *89*, 2896.
(9) Kato, S.; Jobe, D.; Rao, N. P.; Ho, C. H.; Verrall, R. E. *J. Phys. Chem.* **1986**, *90*, 4167.
(10) Borthakur, A.; Zana, R. *J. Phys. Chem.* **1987**, *91*, 5957.
(11) D'Arrigo, G.; Paparelli, A. *J. Chem. Phys.* **1989**, *91*, 2587.
(12) Baaken, C.; Belkoura, L.; Fusenig, S.; Müller-Kirschbaum, Th., Woermann, D. *Ber. Bunsen-Ges. Phys. Chem.* **1990**, *94*, 150.
(13) Frindi, M.; Michels, B.; Zana, R. *J. Phys. Chem.* **1992**, *96*, 6095.
(14) Kaatze, U.; Menzel, K.; Schwerdtfeger, S. *Z. Phys. Chem.* **1994**, *186*, 141.
(15) Eggers, F.; Kaatze, U. *Meas. Sci. Technol.* **1996**, *7*, 1.
(16) Kaatze, U.; Wehrmann, B.; Pottel, R. *J. Phys. E: Sci. Instrum.* **1987**, *20*, 1025.
(17) Labhardt, A. M. Dissertation, Universität Basel, Basel, 1975.
(18) Labhardt, A. M.; Schwarz, G. *Ber. Bunsen-Ges. Phys. Chem.* **1976**, *80*, 83.
(19) Menzel, K. Dissertation; Georg-August-Universität, Göttingen, 1993.
(20) Kaatze, U.; Kühnel, V.; Menzel, K.; Schwerdtfeger, S. *Meas. Sci. Technol.* **1993**, *4*, 1257.
(21) Kaatze, U.; Lautscham, K.; Brai, M. *J. Phys. E: Sci. Instrum.* **1988**, *21*, 98.
(22) Bömmel, H. E.; Dransfeld, K. *Phys. Rev. Lett.* **1958**, *1*, 234.
(23) Kaatze, U.; Kühnel, V.; Weiss, G. *Ultrasonics* **1996**, *34*, 51.
(24) Khimunin, A. S. *Acustica* **1972**, *27*, 173.
(25) Fay, B. *Acustica* **1976/1977**, *36*, 209.
(26) Riech, M. Diploma Thesis; Georg-August-Universität, Göttingen, 1996.
(27) Kahlweit, M.; Busse, G.; Jen, J. *J. Phys. Chem.* **1991**, *95*, 5580.
(28) Zielesny, A.; Schmitz, J.; Limberg, S.; Aizpiri, A. G.; Fusenig, S.; Woermann, D. *Int. J. Thermophys.* **1994**, *15*, 67.
(29) Debye, P. *Polare Molekeln*; Hirzel: Leipzig, 1929.
(30) Marquardt, D. W. *J. Soc. Ind. Appl. Math.* **1963**, *2*, 2.
(31) Hill, R. M. *Nature* **1978**, *275*, 96.
(32) Hill, R. M. *Phys. Status Solidi* **198**, *103*, 319.
(33) Rupprecht, A.; Menzel, K.; Kühnel, V.; Kaatze, U. *J. Acoust. Soc. Am.*, in preparation.
(34) Allegra, J. R.; Hawley, S. A. *J. Acoust. Soc. Am.* **1972**, *51*, 1545.
(35) Ahuja, A.; Hendee, W. R. *J. Acoust. Soc. Am.* **1978**, *63*, 1074.
(36) Davis, M. C. *J. Acoust. Soc. Am.* **1979**, *65*, 387.
(37) McClements, D. J. *J. Acoust. Soc. Am.* **1992**, *91*, 849.
(38) Kaatze, U.; Trachimow, C.; Pottel, R.; Brai, M. *Ann. Phys. Heidelberg* **1996**, *5*, 13.
(39) Fixman, M. *J. Chem. Phys.* **1960**, *33*, 1364.
(40) Fixman, M. *Adv. Chem. Phys.* **1964**, *4*, 175.
(41) Romanov, V. P.; Solov'ev, V. A. *Sov. Phys. Acoust.* **1965**, *11*, 68.
(42) Romanov, V. P.; Solov'ev, V. A. *Sov. Phys. Acoust.* **1965**, *11*, 219.
(43) Isakovich, M. A.; Chaban, I. A. *Zh. Eksp. Teor. Fiz.* **1966**, *23*, 893.
(44) Solov'ev, V. A.; Montrose, C. J.; Watkins, M. H.; Litovitz, T. A. *J. Chem. Phys.* **1968**, *48*, 2155.
(45) Kawasaki, K. *Phys. Rev. A* **1970**, *1*, 1750.
(46) Kroll, D.; Ruhland, J. *Phys. Lett. A* **1981**, *80*, 45.
(47) Bhattacharjee, J. K.; Ferrell, R. A. *Phys. Rev. A* **1981**, *24*, 1643.
(48) Kawasaki, K.; Shiwa, Y. *Physica A* **1982**, *113*, 27.
(49) Ferrell, R. A.; Bhattacharjee, J. K. *Phys. Rev. A* **1985**, *31*, 1788.

(50) Endo, H. *J. Chem. Phys.* **1990**, *92*, 1986.
(51) Kühnel, V.; Kaatze, U. *J. Phys. Chem.* 1996, in press.
(52) Egelstaff, P. A. *An Introduction to the Liquid State*; Academic: New York, 1967.
(53) Chudley, C. T.; Elliott, R. J. *Proc. Phys. Soc., London* **1960**, *77*, 353.
(54) Kato, T. *J. Phys. Chem.* **1985**, *89*, 5750.
(55) Bender, T. M.; Pecora, R. *J. Phys. Chem.* **1988**, *92*, 1675.
(56) Castillo, R. C.; Domingues, H. C.; Costas, M. *J. Phys. Chem.* **1990**, *94*, 8731.
(57) Quirion, F.; Magid, L. F.; Drifford, M. *Langmuir* **1990**, *6*, 244.
(58) Aizpiri, A. G.; Monroy, F.; del Campo, C.; Rubio, R. G.; Diaz Peña, M. *Chem. Phys.* **1992**, *165*, 31.
(59) Lara, J.; Desnoyers, J. E. *J. Solution Chem.* **1981**, *10*, 465.
(60) Roux, G.; Perron, G.; Desnoyers, J. E. *J. Solution Chem.* **1978**, *7*, 639.
(61) Kaatze, U.; Schreiber, U. *Chem. Phys. Lett.* **1988**, *148*, 241.
(62) Gailus, T. Dissertation; Georg-August-Universität, Göttingen, 1996.
(63) Strehlow, H.; Knoche, W. *Fundamentals of Chemical Relaxation*; Verlag Chemie: Weinheim, 1977.
(64) Kaatze, U.; Lautscham, K.; Berger, W. *Chem. Phys. Lett.* **1988**, *144*, 273.
(65) Davis, C. M.; Jarzynski, J. In *Water, a Comprehensive Treatise*; Franks, F., Ed.; Plenum: New York, 1972; Vol. 1, p 443.
(66) Litovitz, T. A.; Davis, C. M. In *Physical Acoustics*; Mason, W. P., Ed.; Academic: New York, 1965; Vol. 2A, p 282.
(67) Madigosky, W. M.; Warfield, R. W. *J. Chem. Phys.* **1983**, *78*, 1912.
(68) Madigosky, W. M.; Warfield, R. W. *Acustica* **1984**, *55*, 123.
(69) Kaatze, U.; Pottel, R.; Schumacher, A. *J. Phys. Chem.* **1992**, *96*, 6017.
(70) Kaatze, U.; Gabriel, B.; Pottel, R. *Ber. Bunsen-Ges. Phys. Chem.* **1994**, *98*, 9.
(71) Kaatze, U.; Kettler, M.; Pottel, R. *J. Phys. Chem.* **1996**, *100*, 2360.
(72) Behrends, R. Diploma Thesis; Georg-August-Universität, Göttingen, 1995.
(73) Behrends, R., unpublished results of this laboratory.